

Twist-Grain Boundary Phase and Blue Phases in Isocyanide Gold(I) Complexes

Rocío Bayón, Silverio Coco, and Pablo Espinet*

Departamento de Química Inorgánica, Facultad de Ciencias, Universidad de Valladolid, E-47005 Valladolid, Spain

Received March 6, 2002. Revised Manuscript Received June 3, 2002

Stable and structurally simple chiral tetrafluorophenyl-gold(I) isocyanide complexes $[\text{Au}(\text{C}_6\text{F}_4\text{OR}^1)(\text{C}\equiv\text{NC}_6\text{H}_4\text{C}_6\text{H}_4\text{OR}^2)]$ [$\text{R}^1 = (\text{R})$ -2-butyl, $\text{R}^2 = \text{C}_n\text{H}_{2n+1}$ ($n = 2, 10$); $\text{R}^1 = \text{C}_m\text{H}_{2m+1}$ ($m = 2, 10$), $\text{R}^2 = (\text{R})$ -2-butyl; $\text{R}^1 = \text{R}^2 = (\text{R})$ -2-butyl] displaying a twist-grain boundary phase (TGBA*) and blue phases are described. Their mesogenic behavior is discussed and their thermal properties are easily tuned by changing the number and position of the chiral chain in the complexes.

Introduction

Chirality in functional molecular materials is a powerful tool for inducing properties and molecular organizations absent in nonchiral materials. This is particularly true in mesogenic materials. For instance, both the twist-grain boundary (TGB) and the blue (BP) phases are two types of frustrated phases with fascinating physical and structural features, which are found exclusively in optically active systems.¹ Although many organic compounds displaying TGB^{2–6} and BPs^{7–11} have been reported, examples of metallomesogens displaying these kind of phases are very scarce.^{12–17} In fact, only two palladium orthometalated complexes showing blue phases¹⁸ and one ferrocene-based Schiff's base derivative displaying both a twist-grain boundary phase (TGBA*) and a blue phase have been reported.¹⁹ Previous works on isocyanide gold(I) complexes showed that the coordinatively simple mesogenic system $[\text{AuX}(\text{CNR})]$ ($\text{X} =$ anionic ligand) is particularly suitable for studying

the effect of structural modifications on the liquid-crystal behavior of the material.^{20–26} We therefore decided to study the influence of introducing one or two chiral centers in gold(I) isocyanide complexes $[\text{Au}(\text{C}_6\text{F}_4\text{OR}^1)(\text{C}\equiv\text{NC}_6\text{H}_4\text{C}_6\text{H}_4\text{OR}^2)]$. This afforded examples of metallomesogens presenting cholesteric phases as well as rare twist-grain boundary and blue phases.

Experimental Section

Combustion analyses were made with a Perkin-Elmer 2400 microanalyzer. IR spectra (cm^{-1}) were recorded on a Perkin-Elmer FT 1720X instrument and ^1H and ^{19}F NMR spectra on Bruker AC 300 or ARX 300 instruments in CDCl_3 . Microscopy studies were carried out using a Leica DMRB microscope equipped with a Mettler FP82HT hot stage and a Mettler FP90 central processor, at a heating rate of $10\text{ }^\circ\text{C min}^{-1}$. For differential scanning calorimetry (DSC) a Perkin-Elmer DSC7 instrument was used, which was calibrated with water and indium; the scanning rate was $10\text{ }^\circ\text{C min}^{-1}$, the samples were sealed in aluminum capsules in the air, and the holder atmosphere was dry nitrogen.

Literature methods were used to prepare $[\text{C}\equiv\text{NC}_6\text{H}_4\text{C}_6\text{H}_4\text{OC}_n\text{H}_{2n+1}]^{22}$ and $[\text{AuCl}(\text{tht})]$ ($\text{tht} =$ tetrahydrothiophene).²⁷

The new chiral isocyanide ligand was prepared from a chiral nitro precursor, as described for similar phenyl isocyanides.²⁸ The chiral chain was introduced, either in $\text{HO}-\text{C}_6\text{H}_4-\text{C}_6\text{H}_4-\text{NO}_2$ or in $\text{HO}-\text{C}_6\text{F}_4-\text{H}$, using the Mitsunobu reaction with (*S*)-2-butanol (Aldrich), triphenylphosphine, and diethyl azodicarboxylate to give the (*R*)-2-butyl derivatives.²⁹

* To whom correspondence should be addressed. E-mail: espinet@qi.uva.es.

- (1) Goodby, J. W. *J. Mater. Chem.* **1991**, *1*, 307.
- (2) Slaney, A. J.; Goodby, J. W. *J. Mater. Chem.* **1991**, *1*, 5.
- (3) Nguyen, H. T.; Bouchta, A.; Navailles, L.; Barois, P.; Isaert, N.; Tweig, R. J.; Maaroufi, A.; Destrade, C. *J. Phys. II Fr.* **1992**, *2*, 1889.
- (4) Navailles, L.; Nguyen, H. T.; Barois, P.; Destrade, C.; Isaert, N. *Liq. Cryst.* **1993**, *15*, 479.
- (5) Nguyen, H. T.; Destrade, C.; Parneix, J. P.; Pochat, P.; Isaert, G.; Girold, N. C. *Ferroelectric* **1993**, *147*, 181.
- (6) Slaney, A. J.; Goodby, J. W. *J. Mater. Chem.* **1995**, *5*, 663.
- (7) Crooker, P. P. *Liq. Cryst.* **1989**, *5*, 751.
- (8) Seidemann, T. *Rep. Prog. Phys.* **1990**, *53*, 659.
- (9) Kitzerow, H. S. *Mol. Cryst. Liq. Cryst.* **1991**, *202*, 51.
- (10) Crooker, P. P.; Kitzerow, H.-S. *Condens. Matter News* **1992**, *1*, 6.
- (11) Heppke, G.; Krüerke, D.; Löhning, C.; Löttsch, D.; Moro, D.; Müller, M.; Sawade, H. *J. Mater. Chem.* **2000**, *10*, 2657.
- (12) Espinet, P.; Esteruelas, M. A.; Oro, L. A.; Serrano, J. L.; Sola, E. *Coord. Chem. Rev.* **1992**, *117*, 215.
- (13) Bruce, D. W. In *Inorganic Materials*, 2nd ed.; Bruce, D. W., O'Hare, D., Eds.; Wiley: Chichester, 1996; Chapter 8.
- (14) *Metallomesogens*; Serrano, J. L., Ed.; VCH: Weinheim, 1996.
- (15) *Handbook of Liquid Crystals*; Demus, D., Goodby, J., Gray, G. W., Spiess, H. W., Vill, D. V., Eds.; Wiley-VCH: Weinheim, 1998.
- (16) Donnio, B.; Bruce, D. W. *Struct. Bonding* **1999**, *95* (Liquid Crystals II), 193.
- (17) Espinet, P. *Gold Bull.* **1999**, *32*, 127.
- (18) Bruce, D. W. *Adv. Inorg. Chem.* **2001**, *52*, 151.
- (19) Seshadri, T.; Haupt, H.-J. *Chem. Commun.* **1998**, 735.

(20) Buey, J.; Espinet, P.; Kitzerow, H.-S.; Strauss, J. *Chem. Commun.* **1999**, 441.

(21) Kaharu, T.; Ishii, R.; Takahashi, S. *J. Chem. Soc., Chem. Commun.* **1994**, 1349.

(22) Benouazzane, M.; Coco, S.; Espinet, P.; Martín-Álvarez, J. M. *J. Mater. Chem.* **1995**, *5*, 441.

(23) Coco, S.; Espinet, P.; Falagán, S.; Martín-Álvarez, J. M. *New J. Chem.* **1995**, *19*, 959.

(24) Benouazzane, M.; Coco, S.; Espinet, P.; Martín-Álvarez, J. M. *J. Mater. Chem.* **1999**, *9*, 2327.

(25) Bayón, R.; Coco, S.; Espinet, P.; Fernández-Mayordomo, C.; Martín-Álvarez, J. M. *Inorg. Chem.* **1997**, *36*, 2329.

(26) Omenat, A.; Serrano, J. L.; Sierra, T.; Amabilino, D. B.; Minquet, M.; Ramos, E.; Veciana, J. *J. Mater. Chem.* **1999**, *9*, 2301.

(27) Usón, R.; Laguna, A.; Vicente, J. *J. Organomet. Chem.* **1977**, *131*, 471.

(28) Coco, S.; Espinet, P.; Martín-Álvarez, J. M.; Levelut, A. M. *J. Mater. Chem.* **1997**, *7*, 19.

(29) Mitsunobu, O. *Synthesis* **1981**, 1.

Only example procedures are described as the syntheses were similar for the rest of the compounds. Yields, IR, and analytical data are given for all the gold complexes.

Preparation of (*R*)-4-(2-Butyloxy)-4'-isocyanobiphenyl.

To a solution of (*R*)-4-(2-butyloxy)-4'-formamidobiphenyl (1.90 g, 7.0 mmol), prepared by reaction of the amine with formic acid,²⁸ and triethylamine 6.00 mmol in 60 mL of CH₂Cl₂ was added dropwise a solution of triphosgene (0.7 g, 2.35 mmol) in 10 mL of CH₂Cl₂. The mixture was stirred for 1 h and then the solvent was removed on a rotary evaporator. The resulting residue was chromatographed (silica gel, CH₂Cl₂/hexane, 4:1 as eluent) and the solvent was evaporated to obtain the product as a cream solid. Yield: 1.45 g, 82%. mp 54 °C. IR $\nu(\text{C}\equiv\text{N})/\text{cm}^{-1}$: (CH₂Cl₂) 2127. ¹H NMR (CDCl₃): δ_1 7.55, δ_2 7.40, AA'XX' spin system ($^3J_{1,2} + ^5J_{1,2'} = 8.6$ Hz), δ_3 7.48, δ_4 6.96, AA'XX' spin system ($^3J_{3,4} + ^5J_{3,4'} = 8.8$ Hz), 4.35 (tq, $J_{\text{CH}-\text{CH}_3} = J_{\text{CH}-\text{CH}_2} = 6.0$ Hz, O-CH), 1.78–1.65 (m, 2H, CH₂), 1.32 (d, $J = 6.0$, CH-CH₃), 0.99 (t, $J = 7.4$, CH₂-CH₃). [α]₅₈₉²⁵ (M = 1, CH₂Cl₂) = -24.1.

Preparation of 1-Decyloxy-2,3,5,6-tetrafluorobenzene.

Anhydrous K₂CO₃ (0.787 g, 5.69 mmol) was added to a solution of 2,3,5,6-tetrafluorophenol (0.700 mL, 3.79 mmol) and 4.170 mmol of bromodecane in 80 mL of dry acetone. The resulting suspension was refluxed under N₂ for 48 h and then allowed to cool to room temperature. The reaction mixture was poured into 200 mL of H₂O and the solution was acidified with diluted HCl. CH₂Cl₂ was added to this mixture, the organic layer was separated, dried over MgSO₄, and filtered, and the solvent was evaporated on a rotary evaporator. The residue was chromatographed (silica gel, hexane as eluent) and the hexane was evaporated to obtain the product as a colorless liquid (95%). ¹H NMR (CDCl₃): δ 6.74 (m, HC₆F₄), 4.21 (t, $J = 0.9$ Hz, CH₂O), 1.86–0.88 (m, 19 H, alkyl chain). ¹⁹F NMR (CDCl₃): δ_1 -156.40 (m, F_{ortho}), δ_2 -157.55 (m, F_{meta}), AA'BB'X spin system.

Ethoxy derivatives were prepared similarly using *N,N*-dimethylformamide as the solvent and refluxing the suspension for 1 h.

Preparation of [Au(C₆F₄OR¹)(C≡NC₆H₄C₆H₄OR²)]. To a solution of HC₆F₄OR¹ (0.312 mmol) in 25 mL of dried diethyl ether was added a solution of LiBu in hexane (0.194 mL, 0.312 mmol) at -78 °C, under nitrogen. After the solution was stirred for 1 h at -50 °C, solid [AuCl(tht)] (0.96 g, 0.312 mmol) was added at -78 °C and the reaction mixture was slowly brought to room temperature (3 h). Then, a few drops of water were added and the solution was filtered in air through anhydrous MgSO₄. C≡NC₆H₄C₆H₄OR² (0.312 mmol) was added to the solution obtained. After the solution was stirred for 15 min, the solvent was removed on a rotary evaporator and the white solid obtained was recrystallized from dichloromethane/hexane at -15 °C.

Yields, IR, and analytical data are as follows:

R¹ = (R)-2-Butyl, R² = C₂H₅. Yield: 46%. IR $\nu(\text{C}\equiv\text{N})$: (CH₂-Cl₂) 2214, (Nujol) 2213. Anal. Calcd for C₂₅H₂₂AuF₄NO₂: C, 46.82; H, 3.46; N, 2.18. Found: C, 46.60; H, 3.46; N, 2.08. [α]₅₈₉²⁵ (M = 1, CH₂Cl₂) = -1.8.

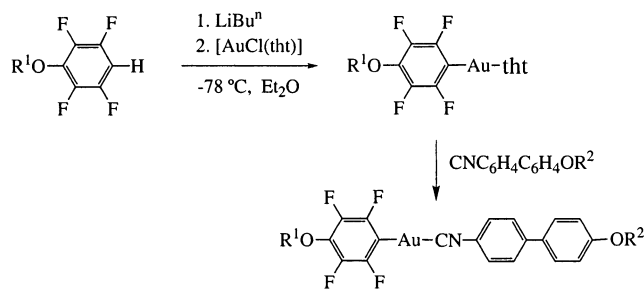
R¹ = (R)-2-Butyl, R² = C₁₀H₂₁. Yield: 40%. IR $\nu(\text{C}\equiv\text{N})$: (CH₂Cl₂) 2214, (Nujol) 2215. Anal. Calcd for C₃₉H₃₈AuF₄NO₂: C, 52.59; H, 5.08; N, 1.86. Found: C, 52.58; H, 4.97; N, 1.61. [α]₅₈₉²⁵ (M = 1, CH₂Cl₂) = -0.8.

R¹ = C₂H₅, R² = (R)-2-Butyl. Yield: 30%. IR $\nu(\text{C}\equiv\text{N})$: (CH₂-Cl₂) 2214, (Nujol) 2216. Anal. Calcd for C₂₅H₂₂AuF₄NO₂: C, 46.82; H, 3.46; N, 2.18. Found: C, 45.54; H, 3.33; N, 2.02. [α]₅₈₉²⁵ (M = 1, CH₂Cl₂) = -8.5.

R¹ = C₁₀H₂₁, R² = (R)-2-Butyl. Yield: 30%. IR $\nu(\text{C}\equiv\text{N})$: (CH₂Cl₂) 2214, (Nujol) 2212. Anal. Calcd for C₃₉H₃₈AuF₄NO₂: C, 52.59; H, 5.08; N, 1.86. Found: C, 52.50; H, 4.88; N, 1.61. [α]₅₈₉²⁵ (M = 1, CH₂Cl₂) = -5.8.

R¹ = R² = (R)-2-Butyl. Yield: 30%. IR $\nu(\text{C}\equiv\text{N})$: (CH₂Cl₂) 2214, (Nujol) 2214. Anal. Calcd for C₂₇H₂₆AuF₄NO₂: C, 48.44; H, 3.91; N, 2.09. Found: C, 48.23; H, 3.80; N, 2.08. [α]₅₈₉²⁵ (M = 1, CH₂Cl₂) = -7.6.

Scheme 1



	R ¹	R ²
1a	(R)-2-butyl	C ₂ H ₅
1b	(R)-2-butyl	C ₁₀ H ₂₁
2a	C ₂ H ₅	(R)-2-butyl
2b	C ₁₀ H ₂₁	(R)-2-butyl
3	(R)-2-butyl	(R)-2-butyl

Results and Discussion

Synthesis and Chemical Characterization. The gold(I) complexes were prepared, as described for similar pentafluorophenyl-gold(I) isocyanide derivatives,²⁵ according to Scheme 1, and were isolated as white solids.

The C, H, and N analyses for the complexes, yields, and relevant IR data are given in the experimental part. The IR spectra are all similar and show one $\nu(\text{C}\equiv\text{N})$ absorption for the isocyanide group at higher wavenumbers (ca. 90 cm⁻¹) than for the free isocyanide, as has been reported for other gold(I) isocyanide compounds.²⁵

The ¹H NMR spectra of the gold(I) isocyanide complexes prepared are all very similar, showing at 300 MHz four somewhat distorted "doublets" for the biphenyl (strictly two AA'XX' spin systems), as we have reported for similar halogold(I) isocyanide complexes.²² In addition, two virtual triplets (quartets for the ethoxy groups) are observed at ca. 4.1 and ca. 3.9 ppm corresponding to first methylene group of the C₆H₄C₆H₄OR² and C₆F₄OR¹ groups, respectively. The remaining chain hydrogens appear in the range 0.8–1.8 ppm.

The ¹⁹F NMR spectra of these complexes show two somewhat distorted "doublets" flanked by two pseudo-triplets corresponding to an AA'XX' spin system with $J_{\text{AA}'} \approx J_{\text{XX}'}$. The signals appear at ca. -118 ppm and ca. -157 ppm (ref. CFCl₃) assigned to $F(\text{ortho})$ and $F(\text{meta})$, respectively, with apparent coupling constants ($N = J_{\text{AX}} + J_{\text{AX}'}$) in the range 18–19.7 Hz.

Mesogenic Behavior. All the complexes prepared display mesomorphic behavior showing mesophases unusually fluid considering that they are metallomesogens (usually metal-containing liquid crystals give mesophases noticeably more viscous than organic liquid crystals). Their optical, thermal, and thermodynamic data are presented in Table 1. For the complexes containing one chiral substituent (**1** and **2**) only a smectic A mesophase is observed when the length of the achiral chain is long (n or $m = 10$, **1b** and **2b** complexes), irrespective of the position of the chiral chain. For shorter alkoxy chains (n or $m = 2$, **1a** and **2a** complexes) both an enantiotropic cholesteric and a monotropic SmA phase are observed. The SmA phase was identified

Table 1. Phase Transition Data for 1, 2, and 3

compound	transition ^a	T(°C)	ΔH(kJ/mol)
1a	C - -N*	134.1	23.30
	N* - -I	189.5	0.60
	I - -N*	183.0	-0.50
	N* - -TGBA- -SmA ^b	116 ^c	
1b	SmA - -C	66.5	-19.80
	C - -SmA	75.5	28.11
2a	SmA - -I	177.9	3.93
	C - -N*	140.3	29.71
2b	N* - -I	150.4	0.54
	I - -N*	149.2	-0.57
	N* - -SmA	116.8	-0.13
	SmA - -C	103.6	-26.13
	C - -C'	3.0	-9.38
	C' - -C''	22.1	-5.12
3	C'' - -SmA	56.2	18.97
	SmA - -I	149.9	3.37
	C - -C'	94.9	0.70
	C' - -I	103.5	22.80
	I-BPIII-BPII-BPI-N* ^b	87.8	-0.31 ^d
N* - -C	76.6	-17.20	
C - -C'	70.4	-0.40	

^a Data refers to the second DSC cycle. ^b Monotropic transition not resolved by DSC. ^c Microscopic data. ^d Combined enthalpies.



Figure 1. Polarized optical microscopic texture of the TGBA* phase of **1a** on heating from homeotropic SmA texture (113.8 °C).

optically by the myelinic and homeotropic textures reorganizing to the fan-shaped texture at temperatures close to the clearing point and the focal-conic fan texture on cooling from the cholesteric or isotropic phases.^{30,31} The cholesteric phases display the Grandjean plane texture. The cholesteric range is clearly higher for **1a**, where the chiral substituent is in the tetrafluorophenyl group. A TGBA* phase, which was identified by their filament texture (Figure 1),^{2,32,33} was observed for **1a** when the SmA to cholesteric transition was studied, heating slowly (0.5 °C min⁻¹) from the SmA phase. Under similar conditions **2a** did not show a TGBA* phase.

The introduction of a second chiral atom in the system leads to a reduction in the mesogenic properties, and only a monotropic chiral nematic transition is observed for compound **3**. When this compound is cooled from the isotropic liquid state at a cooling rate of 0.5 °C min⁻¹,

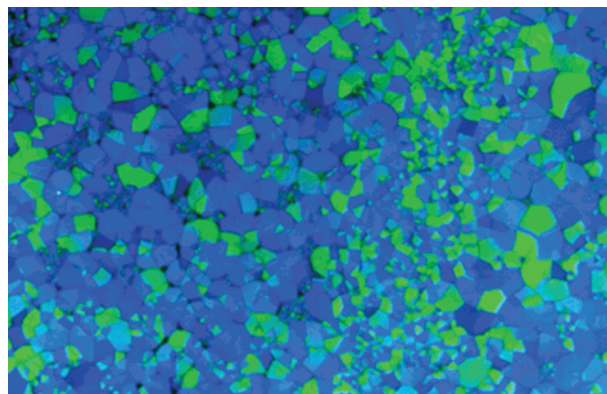


Figure 2. Polarized optical microscopic texture (×100) of the BP-II platelet texture of **3** on cooling from the isotropic liquid (89 °C).

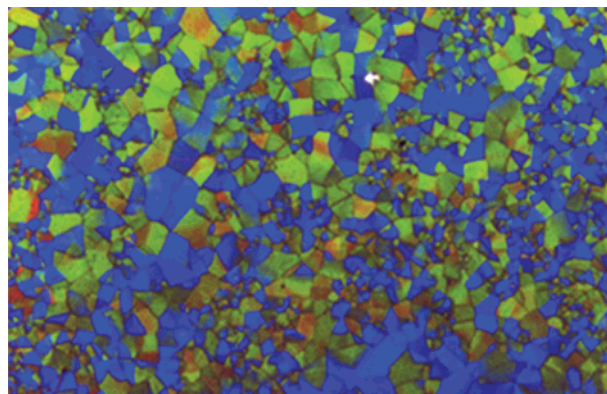


Figure 3. Polarized optical microscopic texture (×100) of the BP-I platelet texture of **3** on cooling from the BP-II (88.6 °C).

blue phases BP-III, BL-II, and BP-I are observed. The BP-III mesophase presents the typical gray texture; the BP-II and BP-I show their platelet texture (Figures 2 and 3).³⁴ In general, blue and TGBA* phases appear when the pitch of the cholesteric phase is relatively short.³⁵ Blue phases usually require pitch values below 500 nm. Hence, the pitch value of the cholesteric phase for **3** must be very short, suggesting that with two chiral carbons shorter pitch values are induced compared to those with just one chiral center in the molecule.

In this respect it is interesting to note that the cholesteric phases displayed by the gold complexes described here, when observed on a microscope operating in reflection mode, show a different selective reflection: Blue for **3**, green for **1a**, and pink for **2a**. Such colors are related to their pitch values and support that these pitch values decrease in the order **3** > **1a** > **2a**.³⁶ Moreover, it is worth noting that **1a**, which has the chiral substituent on the tetrafluorophenyl group, has a shorter pitch than **2a** with the chiral chain placed on the isocyanide ligand. This behavior may be related to the fact that the motion of the chiral carbon is more hindered in the tetrafluorophenyl group (due to the presence of the fluorine substituents in the ortho positions of the tetrafluorophenyl ring) than in the isocyanide ligand.

(30) Gray, G. W.; Goodby, J. W. In *Smeectic liquid crystals*; Leonard Hill: Glasgow and London, 1984.

(31) Demus, D.; Richter, L. In *Textures of liquid crystals*, 2nd ed.; VEB: Leipzig, 1980.

(32) Goodby, J. W.; Wangh, M. A.; Stein, S. M.; Chin, E.; Pindak, R.; Patel, J. S. *Nature* **1989**, *337*, 449.

(33) Gilli, J. M.; Kamaye, M. *Liq. Cryst.* **1992**, *4*, 545.

(34) Stegemeyer, H.; Blümel, T.; Hiltrop, H.; Onusseit, H.; Porsch, F. *Liq. Cryst.* **1986**, *1*, 3.

(35) Slaney, A. J.; Goodby, J. W. *J. Mater. Chem.* **1995**, *5*, 663.

(36) Leder, L. B. *J. Chem. Phys.* **1971**, *55*, 2649.

In summary, stable chiral tetrafluorophenyl–gold(I) isocyanide complexes with a very simple molecular structure show TGBA* and blue phases, which are respectively the second and the fourth and fifth examples of metallomesogens displaying such phases. The mesogenic behavior and the pitch of cholesteric mesophases, which determine the appearance of blue phases or the TGBA* phase, are easily modulated by

variation of the number and position of the chiral centers.

Acknowledgment. This work was sponsored by the Spanish Comisión Interministerial de Ciencia y Tecnología (Project MAT99-0971) and the Junta de Castilla y León (Projects VA15/00B and VA050/02).

CM020246Y